Synthesis, conformational analysis and glycosidase inhibition of bicyclic nojirimycin C-glycosides based on an octahydrofuro[3,2-b]pyridine motif

Jérôme Désiré, Quentin Foucart, Ana Poveda, Gurvan Gourlaouen, Yuna Shimadate, Maki Kise, Cameron Proceviat, Roger Ashmus, David Vocadlo, Jesús Jiménez-Barbero, et al.

Synthesis, conformational analysis and glycosidase inhibition of bicyclic nojirimycin *C*-glycosides based on an octahydrofuro[3,2-b]pyridine motif

Jérôme Désiré,[1]* Quentin Foucart,[1] Ana Poveda,[2] Gurvan Gourlaouen,[1] Yuna Shimadate,[3] Maki Kise,[3] Cameron Proceviat,[4] Roger Ashmus,[4] David J. Vocadlo,[4] J. Jiménez-Barbero,[2] Atsushi Kato[3]* and Yves Blériot[1]*

[1] Université de Poitiers, IC2MP, UMR CNRS 7285, Equipe "Synthèse Organique", Groupe Glycochimie 4 rue Michel Brunet, 86073 Poitiers cedex 9, France; e-mail: yves.bleriot@univ-poitiers.fr; jerome.desire@univ-poitiers.fr

[2] CIC bioGUNE, Parque technologico de Bizkaia, Edif. 801A-1°, Derio-Bizkaia 48160, and Ikerbasque, Basque Foundation for Science, Maria Lopez de Haro 3, 48013 Bilbao, Spain

[3] Department of Hospital Pharmacy, University of Toyama, 2630 Sugitani, Toyama 930-0194, Japan e-mail: kato@med.u-toyama.ac.jp

[4] Department of Chemistry, Simon Fraser University, 8888 University Drive, Burnaby, British Columbia, Canada V5S 1P6

* Correspondence: Jérôme Désiré, E-mail: jerome.desire@univ-poitiers.fr; Yves Blériot, E-mail: yves.bleriot@univ-poitiers.fr; Atsushi Kato, E-mail: kato@med.u-toyama.ac.jp

Abstract: A set of bicyclic iminosugar *C*-glycosides, based on a octahydrofuro[3,2-b]pyridine motif, has been synthesized from a *C*-allyl iminosugar exploiting a debenzylative iodocycloetherification and a iodine nucleophilic displacement as the key steps. The halogen allowed the introduction of a range of aglycon moieties of different sizes bearing several functionalities such as alcohol, amine, amide and triazole. In these carbohydrate mimics the fused THF ring forces the piperidine to adopt a flattened $^1C_4$ conformation according to NMR and DFT calculations studies. In their deprotected form, these bicycles were assayed on a panel of 23 glycosidases. The iminosugars displaying hydrophobic aglycon moieties proved to be superior glycosidase inhibitors, leading to a low micromolar inhibition of human lysosome β-glucosidase (compound **11**; IC_{50} = 2.7 μM) and rice α-glucosidase (compound **10**; IC_{50} = 7.7 μM). Finally, the loose structural analogy of these derivatives with Thiamet G, a potent OGA bicyclic inhibitor, was illustrated by the weak OGA inhibitory activity (Ki = 140 μM) of iminosugar **5**.

Keywords: iminosugar; glycosidase; conformation; inhibition; bicycle, hexosaminidase.

1. Introduction

Carbohydrate-processing enzymes represent an important class of proteins found in nature that are involved in a vast array of biological processes including cell signalling, inflammation and protein quality control [1]. One sub-class of glycosidases of significant interest is constituted by the exo-N-acetyl-D-hexosaminidases (HexNAcase) that process N-acetylglucosamine and N-acetylgalactosamine residues from glycoconjugates. These enzymes are ubiquitous in all domains of life where, for example, they play roles in peptidoglycan recycling [2], bacterial virulence [3], as well as diverse roles in eukaryotic cell physiology [4]. Notably, *N*-acetylhexosaminidases have attracted considerable interest, due to their involvement in diseases such as osteoarthritis [5], allergy [6], as well as Alzheimer's disease [7]. In addition, catalytically inactive and misfolded mutant forms of N-acetylhexosaminidases are responsible for hereditary lysosomal disorders [8] and inhibitors of this class of glycosidases have been suggested as pharmacological chaperone therapeutics for Tay-Sachs' as well as Sandhoff's diseases [9]. Lysosomal HexNAcases are among the glycosidases secreted into extra cellular space by cancer cells to remodel and degrade the extra cellular matrix (ECM), allowing the cancer to spread to secondary locations in a process known as

metastasis formation [10]. Regarding the enzymatic mechanism, as seen for glycosidases in general, N-acetylhexosaminidases from GH3 family [11] carry out glycosidic bond cleavage in which an enzymic catalytic nucleophile attacks the anomeric center to generate a glycosyl enzyme intermediate, which is subsequently broken down by attack of water at the anomeric center. Both steps of this reaction proceed through oxocarbenium ion-like transition states (TS), which are characterized by the development of positive charge at the anomeric carbon and extending to the endocyclic oxygen through lone pair conjugation [12]. However, hydrolysis by N-acetylhexosaminidases from GH84 [13] and from GH20 [14] harnesses a mechanism that differs in the nature of the catalytic nucleophile. For enzymes from these families, the 2-acetamido group provides neighboring group participation and attacks the anomeric carbon to give rise to an oxazoline or oxazolinium ion intermediate (Figure 1B) [12]. Inspired by this distinctive mechanism and of the biological importance of the related enzymes, a vast array of compounds has been designed and tested especially as O-GlcNAcase inhibitors [15]. Amongst them, a set of synthetic bicyclic sugar-derived inhibitors, that are easily accessible by synthesis, have been reported as having down to picomolar K_i values and impressive selectivity toward OGA. The most representative molecules include NAG-thiazoline **1** [16], NButGT **2** [17], commercially available Thiamet G **3** [18], and the recently described MK-8719 **4** [19] that entered Phase I clinical trials with the goal of being developed to treat the neurodegenerative disease progressive supra-nuclear palsy (Figure 1A). In these derivatives, the transient enzyme-bound oxazoline intermediate is efficiently mimicked by the thiazoline or aminothiazoline moiety but the glycosyl oxocarbenium ion like character of the TS, namely the positive charge localized on the endocyclic oxygen of the sugar ring, is not mimicked. In this work, we set out to explore this aspect by reporting the synthesis, conformational examination, and biological evaluation of a series of bicyclic iminosugars **5-11** (Figure 1C). In these sugar analogs the ring oxygen has been replaced by a nitrogen atom, designed to emulate the glycosyl cation-like character of the TS of hexosaminidases, and to enable this the oxazolidine ring has been replaced by a THF ring.

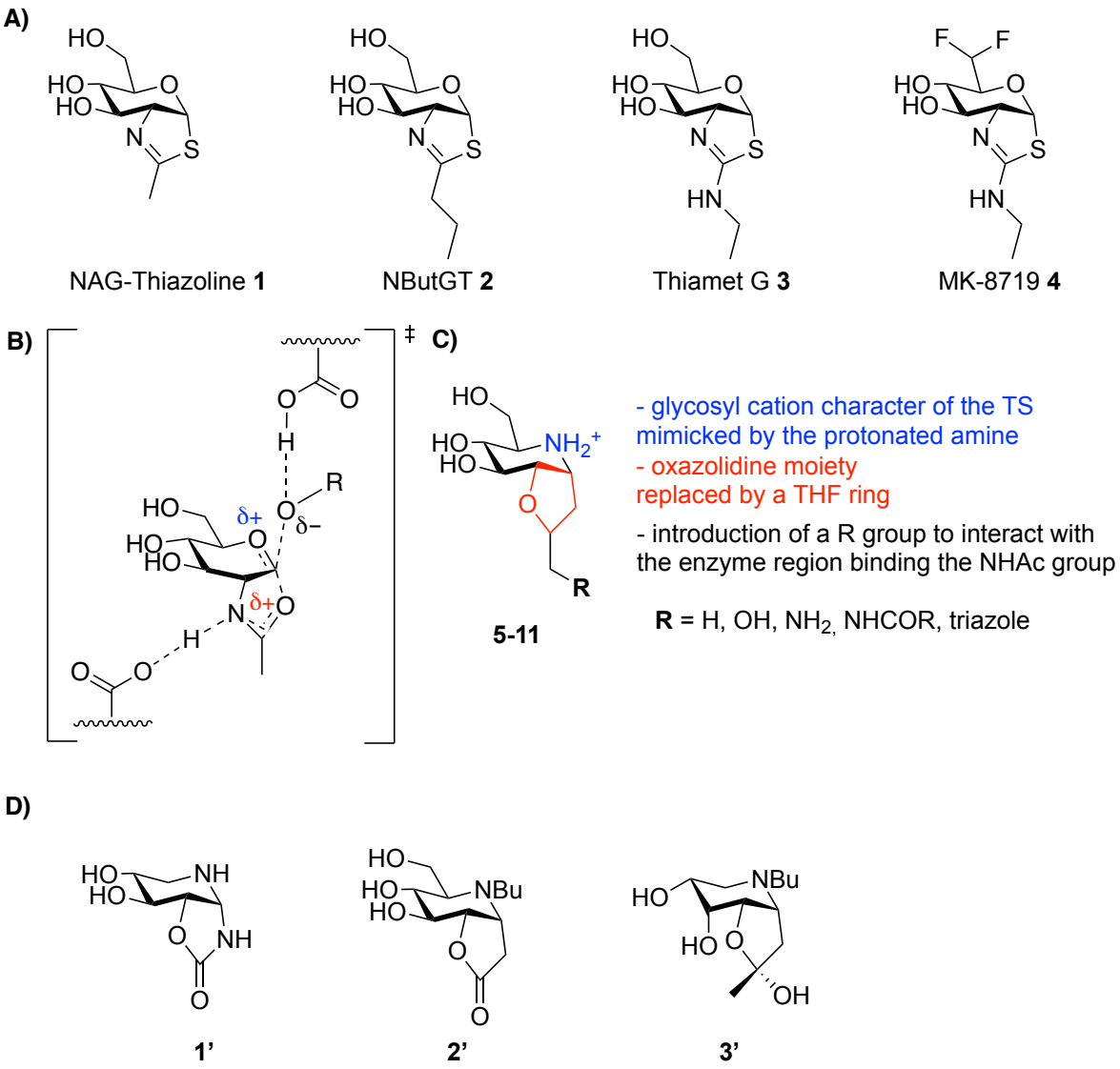

Figure 1. (**A**) Structure of known OGA bicyclic inhibitors **1-4**; B) Proposed transition state (TS) for formation of the oxazoline intermediate; C) Structure of new bicyclic iminosugars **5-11** reported in this study and the rationale for their design; D) Structure of related iminosugars **1'-3'** in the literature.

Addition of a fused five-membered ring to a core monosaccharide motif or analog is a strategy often seen within nature, and exploited by researchers, to generate bicyclic constrained structures that have limited conformational flexibility.[20] Indeed, naturally occurring swainsonine [21] as well as sp^2 iminosugars [22], in which the nitrogen atom is at the junction of the two rings, are well established as valuable tools to study glycoside processing enzymes. Apart from compounds **1-4** reported above, other sugar derivatives that display an extra ring fused to the C1-C2 bond have been synthesized [23] for different purposes ranging from serving as peptide mimics to Tn antigen constrained analogs. Introduction of such structural modification in iminosugars as illustrated by compounds **1'-3'** is scarce (Figure 1D). [24]

2. Results

2.1. Chemistry

2.1.1. Preparation of the bicyclic iminosugar *C*-glycoside scaffold

Two decades ago, the group of Nicotra reported the debenzylative iodocycloetherification [25] of various *C*-allyl glycosides [26]. This transformation, recently used in the total synthesis of herbicidin C [27], allowed access to bicyclic carbohydrate scaffolds in which their rigidity and the ease by which structural elements can be appended to them were notably exploited in the context of generating peptide mimetics [28] and exploring chemical diversity [29]. Applied to the corresponding *C*-allyl iminosugar **B** [30-32] obtained in 60% and six steps from commercially available tetrabenzyl glucose **A**, this reaction yielded the expected bicycle **C** in 47% yield and excellent stereocontrol (Scheme 1).

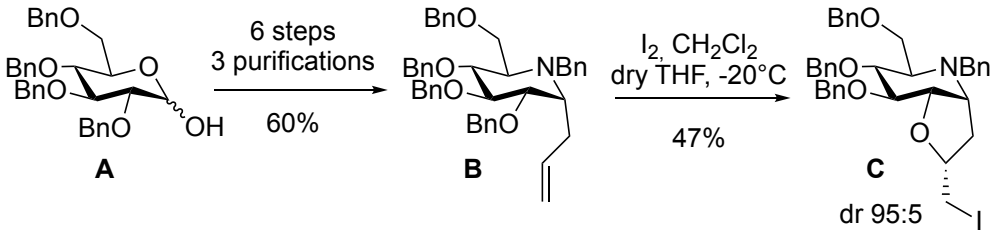

Scheme 1. Synthesis of iodocycloether **C** from commercially available tetrabenzyl glucose **A**.

2.1.2. Synthesis of bicyclic iminosugar *C*-glycosides bearing a methyl or hydroxymethyl appendage

Bicycle **C** is a useful scaffold to generate a small library of bicyclic iminosugars encompassing the suitable hydroxyl pattern and the required positive charge of the TS, as well as a five-membered THF ring. Importantly, tuning of the pK_a of the appendage in the aminothiazoline moiety of Thiamet G **3**, that interact with the enzymatic region that serves to position the 2-acetamido group of the substrate, has been shown to be important to improve the inhibitor potency and selectivity [33]. In this context, the iodine atom in scaffold **C,** through its nucleophilic displacement, should allow the introduction of functional diversity that enables installing groups with a desirbale pK_a value. To this end, the iodocycloether **C** was synthesized on a multigram scale. To test its chemical stability and reactivity, it was first treated with $LiAlH_4$ (4 eq.) in THF at room temperature to furnish the methyl derivative **12** in an unoptimized 32% yield. Its subsequent hydrogenolysis quantitatively yielded the bicyclic iminosugar **5** demonstrating the relative chemical robustness of this bicycle. Introduction of an OH group was achieved by treating **C** with AgOAc (10 eq.) in dry toluene at 50°C for 48 h that furnished the expected ester **13** in 61% yield. Deacetylation with NaOMe in dry MeOH overnight provided the corresponding alcohol that was directly engaged in a hydrogenolysis step to afford the tetrahydroxylated iminosugar **6**. In order to build up a small library of compounds with various aglycon moieties, we relied on the introduction of an azide function that could be then exploited to connect amines and amides but also others functionalities and substituents through the use of click chemistry. Displacement of the iodine atom with NaN_3 at room temperature furnished the key azide **14** in 81% yield (Scheme 2).

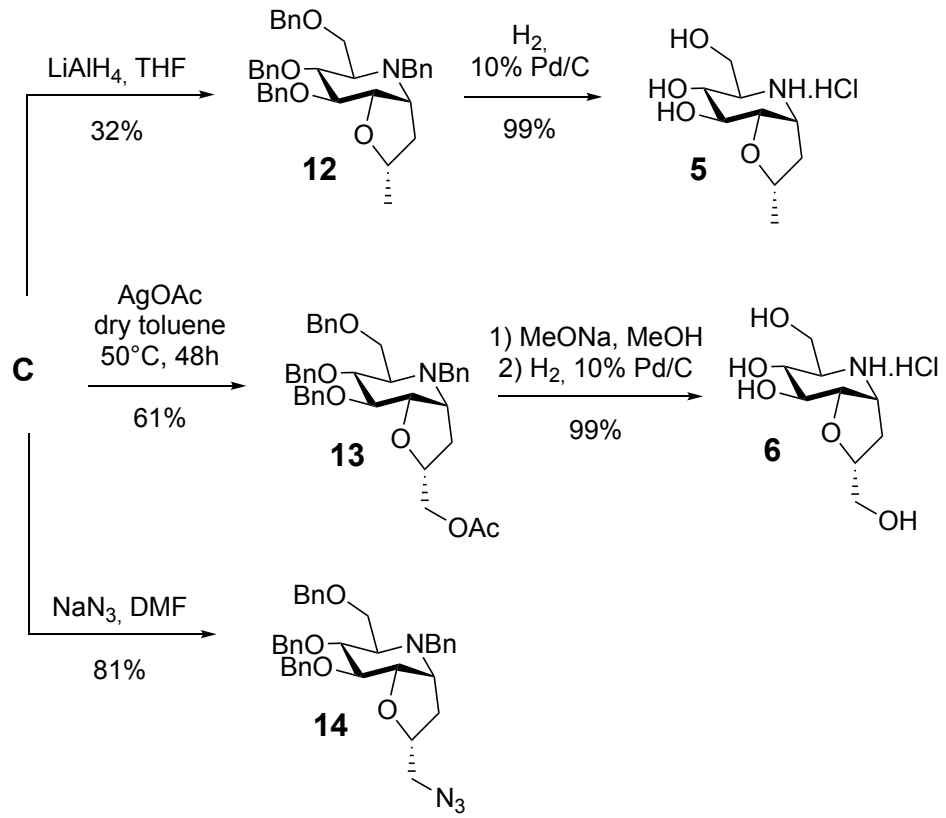

Scheme 2. Synthesis of bicyclic iminosugars **5**, **6** and **14**

2.1.3. Synthesis of bicyclic iminosugar *C*-glycosides bearing amine, amide and triazole appendages

Introduction of an amine and acetamide function was investigated first as these groups could mimic the exocyclic amine found in Thiamet G **3** and MK-8719 **4**. Hydrogenolysis of azide **14** uneventfully yielded the diamine **7**, while its reduction with supported PPh_3 in NH_4OH/THF provided the corresponding crude amine that was directly acetylated with Ac_2O in pyridine to obtain the acetamide **15,** which, upon hydrogenolysis, furnished the iminosugar **8**. Introduction at the C-2 position of amides differing in shape and size has been used in hexosaminidase inhibitors to improve their potency and selectivity by exploiting enzymatic plasticity [34-37]. Thus, reaction of azide **14** respectively with nonyne and 5-phenylpentyne in the presence of 2,6-lutidine and tetrakis(acetonitrile) copper(I) hexafluorophosphate complex furnished the corresponding triazoles **16** and **17** in 50% and 54% yield respectively. Their hydrogenolysis quantitatively yielded the iminosugars **9** and **10.** As these molecules proved to be potent glucosidase inhibitors (vide infra), a derivative bearing a long alkyl chain connected by an amide bond to the bicyclic iminosugar was prepared to check whether the triazole had an influence on the potency of these molecules. Azide **14** was therefore reduced to the crude amine and acylated with nonanoyl chloride in the presence of triethylamine to produce acetamide **18,** which upon deprotection, furnished the iminosugar **11** (Scheme 3).

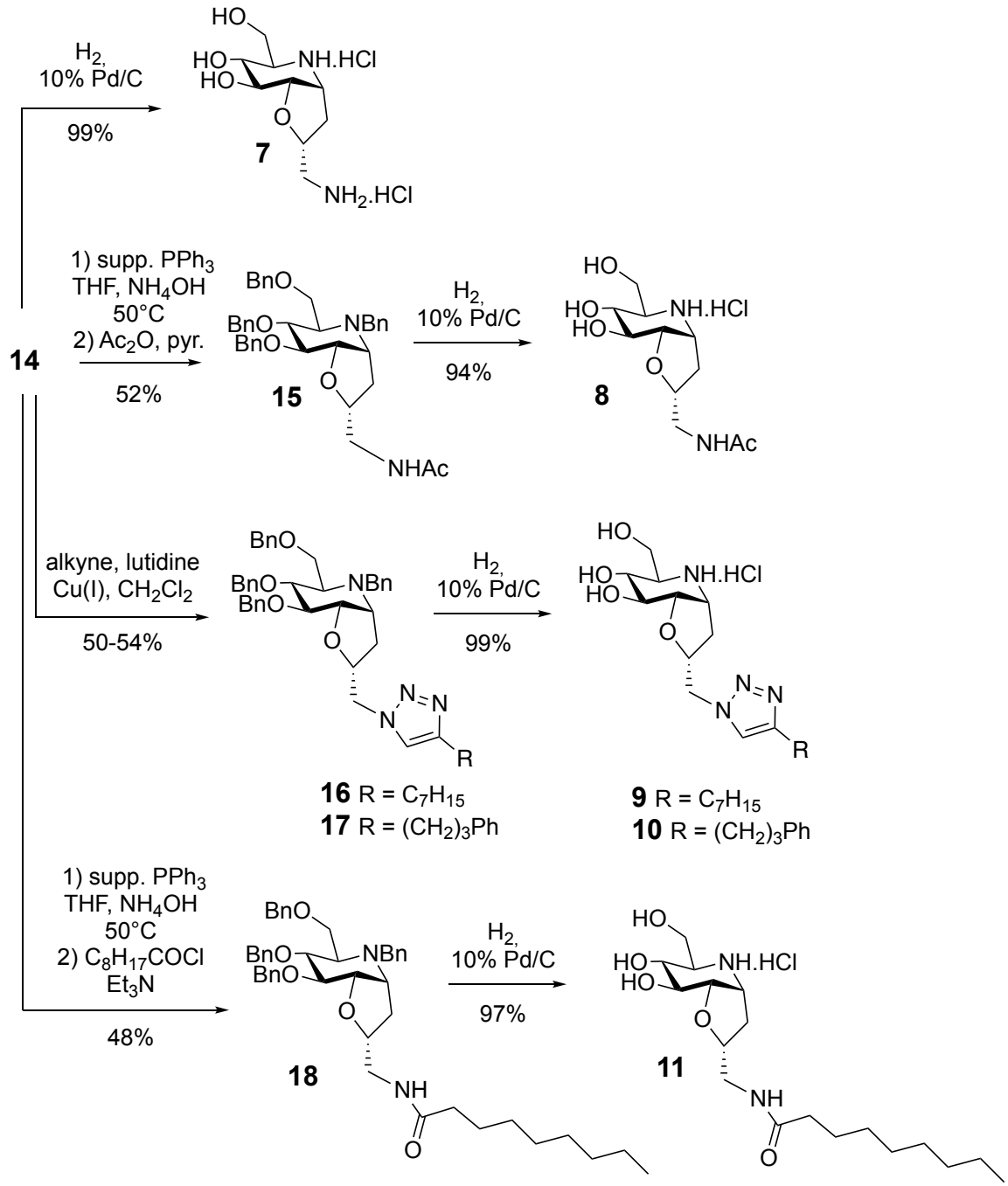

Scheme 3. Synthesis of bicyclic iminosugars **7-11**

2.2. Conformation analysis by NMR and DFT calculations

In order to gain insights into the conformation of the bicyclic iminosugars, including the orientation of the substituent on the THF ring, bicyclic iminosugars **9** and **11** were chosen as representatives of the set of compounds depicted in this study. Conformational analysis of iminosugar **9** by NMR and DFT calculations demonstrated that the iminosugar ring adopt a flattened $^4C_1$ conformation that was, according to NMR data ($^3J_{5,6}$ = 7.9 Hz, $^3J_{6,7}$ = 7.7 Hz, $^3J_{7,7a}$ = 6.2 Hz), close to the slightly distorted $^4C_1$ chair conformation observed for NAG thiazoline in complex with BtGH84 [38] (Figure 2A). Similarly, conformational analysis of iminosugar **11** also demonstrated a chair-like conformation that was somewhat flattened ($^3J_{5,6}$ = 8.4 Hz, $^3J_{6,7}$ = 7.7 Hz, $^3J_{7,7a}$ = 6.2 Hz). The coupling constant ($^3J_{3a,7a}$ =

6.3 Hz) between the protons in the fused ring position is consistent with an eclipsed arrangement of these protons. Typical NOEs crosspeaks between H7 and H5 (equivalent to H3 and H5 in Glc) and between H7a and H6 (similar to H2 and H4 in Glc) are also consistent with a flattened $^{4}C_{1}$ chair conformation. Analysis of HSQC and HMBC spectra for compounds **9** and **11** showed a high degree of similarity, indicating that the carbon skeleton is comparable in both molecules (see SI).

(A) **(B)**

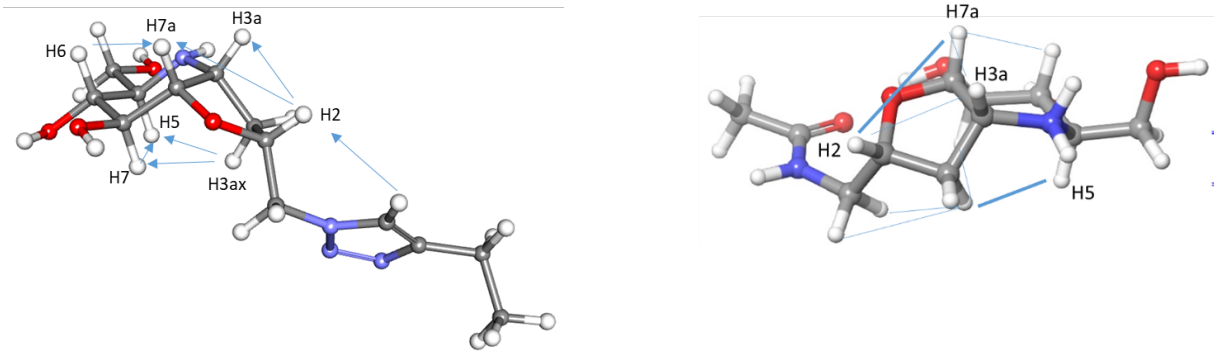

Figure 2. Proposed model for the conformation of iminosugar **9** (A) and iminosugar **11** conformation (B) from DFT calculations in full agreement with the NMR experimental data.

2.3. Glycosidase inhibition by bicyclic nojirimycin C-glycosides

The glycosidase inhibitory potency of these 7 newly synthesized nojirimycin C-glycosides **5-11** were first assayed on a panel of nineteen glycosidases (Table 1). The D-gluco stereochemistry of these molecules was seen to translate into their potent inhibition of α-glucosidase from rice and β-glucosidases from bovine liver and human lysosome. It seems that the incorporation of the 2-OH group of the parent iminosugar in the THF ring conformation is well tolerated by the assayed glucosidases. The simplest bicycle **5** showed moderate inhibition against rice α-glucosidase (IC_{50} 36 μM). Usually, inhibitory potency of both rice α-glucosidase and rat intestinal maltase is closely related and parallel. However, here, the bicyclic molecules show some interesting selectivity toward the rice enzyme. Introduction of an OH function on the methyl group of **5** as in **6** did not significantly modify the inhibition profile. Replacement of the OH group by an amine as in **7** reduced the potency toward rice α-glucosidase (IC_{50} 109 μM). Switching from an amine to an acetamide group as in **8** has no effect on the overall potency. Nevertheless, introduction of bulkier/lipophilic groups as in compounds **9-11** had a significant impact of the inhibition profile of these derivatives. First, replacing the triazole linker present in **9** and **10** by an amide bond as seen in **11** seems to have no effect on the inhibition profile of these molecules. Compounds **9-11** showed increased potency toward rice α-glucosidase (IC_{50} 7.7 μM for compound **10**), but they also displayed significant inhibition of bovine liver β-glucosidase (IC_{50} 4.6 μM for compound **9**) and more importantly of human lysosome β-glucosidase (IC_{50} 2.7 μM for compound **11**), the enzyme whose deficiency is responsible for Gaucher disease [39]. As expected, all compounds showed some inhibition of bovine liver β-galactosidase, culminating in compound **9** (IC_{50} 0.39 μM), an enzyme that is usually strongly inhibited by a range of sugar mimics [40]. Altogether, these preliminary results indicate that fine tuning of the lipophilic moiety in these derivatives might lead to potent and selective β-glucosidase inhibitors. Disappointingly, none of these compounds showed significant inhibition of β-N-acetyl-D-glucosaminidases from bovine kidney, HL60, jack bean, and human recombinant α-N-acetyl-D-glucosaminidase at even a 1 mM concentration.

Table 1. Concentration of iminosugars giving 50 % inhibition of various glycosidases

	IC_{50} (μM)						
Enzyme	**5**	**6**	**7**	**8**	**9**	**10**	**11**
α-Glucosidase							
Yeast	[a]NI [b](23.1%)	540	NI (29.7%)	NI (16.1%)	NI (31.9%)	310	NI (37.8 %)
Rice	36	57	109	82	13	7.7	16.0
Rat intestinal maltase	193	372	155	488	279	154	187
β-Glucosidase							
Almond	NI (22.3%)	NI (21.6%)	NI (15.1%)	NI (19.7%)	NI (31%)	NI (7.9%)	NI (15.7 %)
Bovine liver	438	255	310	NI (46.6%)	4.6	7.6	10
Human lysosome	127	15.9	42.4	NI (0 %)	63.1	6.0	2.7
α-Galactosidase							
Coffee beans	136	NI (3.6%)	NI (24.5%)	NI (4.6%)	NI (1.0%)	NI (5.0%)	NI (0 %)
β-Galactosidase							
Bovine liver	117	83	292	166	0.39	1.1	3.0
α-Mannosidase							
Jack bean	NI (0%)	NI (0%)	NI (2.5%)	NI (0%)	NI (0%)	NI (3.2%)	NI (0 %)
β-Mannosidase							
Snail	ND	NI (0%)	NI (0%)	NI (6%)	NI (25.7%)	NI (35.1%)	NI (12.4 %)
α-L-Fucosidase							
Bovine kidney	NI (0%)	NI (20.1%)	NI (30.6%)	NI (0%)	NI (0%)	NI (0%)	NI (0 %)
α,α-Trehalase							
Porcine kidney	NI (4.0%)	NI (8.8%)	NI (10.7%)	NI (4.0%)	NI (9.1%)	NI (3.6%)	NI (0 %)
Amyloglucosidase							
Aspergillus niger	NI (6.7%)	NI (34.6%)	NI (10.7%)	NI (0%)	NI (27.8%)	NI (23.7%)	NI (29.2 %)
α-L-Rhamnosidase							
Penicillium decumbens	ND	NI (5.1%)	NI (7.0%)	NI (5.7%)	NI (26.4%)	NI (8.3%)	544
β-Glucuronidase							
E.coli	NI (22.9%)	NI (43.4%)	728	NI (1.2%)	813	660	424
Bovine liver	ND	NI (4.4%)	NI (8.1%)	NI (0%)	NI (0%)	NI (0%)	NI (12.5 %)
β-*N* -Acetylglucosaminidase							
Bovine kidney	NI (18.0%)	NI (0%)	NI (3.1%)	NI (0%)	NI (10%)	NI (0%)	NI (5.5 %)
HL60	NI (4.0%)	NI (0%)	NI (0%)	NI (4.4%)	NI (12.4%)	NI (0%)	NI (2.6 %)
Jack bean	NI (25.5%)	NI (0%)	NI (25%)	NI (30%)	NI (31.7%)	NI (15.2%)	NI (34.4 %)
α-*N* -Acetylglucosaminidase							
Human recombinant	NI (31.0%)	NI (34.9%)	NI (13.2%)	NI (0%)	NI (20.8%)	NI (0%)	NI (0%)

[a] NI: No inhibition (less than 50% inhibition at 1000 μM).
[b] ( ): inhibition % at 1000 μM.

Table 1. Concentration of iminosugars giving 50% inhibition of various glycosidases.

2.4. Human and bacterial N-acetyl-D-glucosaminidase inhibition by bicyclic nojirimycin C-glycosides

While nojirimycin *C*-glycosides **5-11** showed no significant inhibition of plant and mammalian hexosaminidases, we have previously observed that poor inhibitors of these enzymes can nevertheless be more potent inhibitors of human and bacterial hexosaminidases [41]. Thus a selection of the nojirimycin *C*-glycosides was assayed as inhibitors of OGA, NagZ, Hex A and HexB enzymes.

Table 2. Concentration of iminosugars giving 50% inhibition

Enzyme/compound	**5**	**7**	**8**	**9**	**10**	**11**
OGA	140	ND	NI	204	NI	488
NagZ	N	NI	NI	NI	405	ND
HexA	NI	NI	NI	NI	NI	ND
HexB	ND	362	459	298	134	NI

The weak inhibitory activity of these compounds reveals certain constraints with regard to the active sites of these enzymes. In particular, OGA, HexA, and HexB all have tightly constrained

active sites in which the acetamido group is carefully packed within a tightly defined pocket, and polarized by an important enzymic catalytic carboxylate that hydrogen bonds with the amide nitrogen of the acetamido group of natural substrates. The THF derivatives (**5**, **7-11**) described here do not enable this hydrogen bond, supporting the importance of this interaction. Moreover, the elaboration of these derivatives with larger substituents is clearly not well tolerated by these enzymes because of the constrained active site pocket. The weak inhibition against NagZ can also be understood in the context of the catalytic mechanism and is also consistent with NAG-Thiazoline being a poor inhibitor of this enzyme [42]. For NagZ enzymes the 2-acetamido group acts as a spectator and larger N-acyl groups are generally well tolerated by a much larger active site that allows substituents to project out into bulk water. The amide moiety, however, hydrogen bonds with a conserved arginine that drive the N-acyl substituent into an orientation that is in plane with the carbohydrate-derived ring [43]. This orientation also enables the enzyme catalytic carboxylate to be positioned below the plane of the sugar ring, directly beneath the anomeric center. Accordingly, the compounds evaluated here, in which the THF ring occupies a space below the piperidine ring and the substituent is oriented in a more downward manner, are likely weak inhibitors because they cannot conform to the requirements of the active site of NagZ. Whilst these compounds are weak inhibitors, their failure to inhibit provides insight into key design features and suggests structures that could be much more potent – in particular we reason that installation of a cyclic amidine in place of the THF moiety could yield very potent inhibition of GH20 and GH84 enzymes and that small N-alkyl substituents on the exocyclic nitrogen could confer selectivity for GH84 enzymes over GH20 enzymes, in keeping with previous reports where such subtle differences have delivered excellent selectivities [17, 19, 33]

3. Conclusion

A small set of constrained nojirimycin C-glycosides **5-11** has been synthesized and evaluated for glycosidase inhibition. The incorporation of the 2-OH group of the nojirimycin scaffold into a fused THF ring still maintains the inhibitory potency of these molecules, some demonstrating low micromolar inhibition toward rice α- and human lysosome β-glucosidase in agreement with their D-gluco like stereochemistry. The initial hypothesis that such bicycles, lacking the key NHAc group or oxazolidine ring, could mimick the overall charge and shape of the OGA TS was supported to some extend as compound **5** proved to be a weak OGA inhibitor. Nevertheless, this poor inhibitor compared to known potent OGA inhibitors emphasizes the necessity to incorporate a NHAc or oxazolidine surrogate in these molecules to reach high potency. All told, the straightforward access to iminosugar C-glycoside scaffold **C** depicted herein is likely to offer opportunities for the preparation of a larger range of iminosugar-derived bicycles displaying other stereochemistries and substitution pattern [32a] that could be of further therapeutic interest [44]. In addition, the iodine atom should be useful to explore other coupling reactions to increase the scope of aglycons to be introduced. Replacement of the THF ring in these derivatives by a pyrrolidine ring is also worth investigating. Work in this direction is in progress in the laboratory.

4. Experimental

General methods: All commercial reagents were used as supplied. TLC plates were visualized under 254 nm UV light and/or by dipping the TLC plate into a solution of phosphomolybdic acid in

ethanol (3 g/100 mL) followed by heating with a heat gun. Flash column chromatography was performed using silica gel 60 (15-40 μm) or carried on a Combiflash® Rf automated apparatus (Teledyne-Isco) using columns specified in each protocol. NMR experiments were recorded with a 400 or 500 Bruker spectrometer at 400 or 500 MHz for ^{1}H and 100 or 125 MHz for ^{13}C nuclei. The chemical shifts are expressed in part per million (ppm) relative to TMS (δ = 0 ppm) and the coupling constant J in hertz (Hz). NMR multiplicities are reported using the following abbreviations: b = broad, s = singulet, d = doublet, t = triplet, q = quadruplet, m = multiplet. HRMS were obtained with a Q-TOF spectrometer from the Mass Spectrometry Service (IC2MP, UMR CNRS 7285-Poitiers University, France). Optical rotations were measured using a Modular Circular Polarimeter MCP100 (Anton Paar).

Conformational analysis: Structural models for compounds **9** and **11** (see supplementary material) were calculated with the Macromodel application within the Maestro software (version 12.3). An initial structure was minimized using conjugate gradients with the OPSL3* force field. A maximum number of 5000 iterations were employed with the PRCG scheme, until the convergence energy threshold was 0.05. The minimized structure was submitted to a conformational search protocol, using a Monte Carlo torsional sampling method (MCMM) with automatic setup during the calculation, energy window of 50 kJ mol-1, 1000 maximum number of steps, and 100 steps per torsion of the bond to be rotated.

Glycosidase assays: Glycosidase inhibition profiling was performed using appropriate *p*-nitrophenyl glycosides as substrates at the optimum pH of each enzyme. The reaction was stopped by adding 400 mM of Na_2CO_3. The released *p*-nitrophenol was measured spectrometrically at 400 nm.

Hexosaminidases assays:

HEXA: IC50 values for compounds against Recombinant Human Hexosaminidase A (HexA) enzyme, purchased from R&D Systems (cat# 6237-GH-020), were determined by measuring the fluorescent signal corresponding to the rate of hydrolytic activity against the commercially available artificial substrate, 4-Methylumbelliferone-N-acetyl-β-D-glucosaminide. HexA inhibition assays were performed in a buffer of 100mM sodium citrate, 250 NaCl, pH 4.5 and 1.0nM [HexA], then stopped after 20 minutes with a solution of 1.0M Tris, pH 9.5 to enhance fluorescent signal. Preliminary experiments have shown that reaction rates are linear for 20 minutes after substrate addition, and that 1.0M Tris at pH 9.5 is sufficient for stopping enzyme activity, as the signal is stable for 24 hours after stopping. Inhibition assays were run in the presence or absence of various concentrations of compounds and at a fixed substrate concentration of 100μM and 1% DMSO. First, compounds were serially diluted to the desired range of concentrations in 2% DMSO buffer. Next, 25μL of compound solutions at various concentrations in 2% DMSO Buffer was added to 25μL of 4.0nM enzyme and allowed to incubate at 25°C for 5 minutes. 50μL of 200μM and 1% DMSO substrate was then added and allowed to react for 20 minutes. 100μL of stop solution was added to reaction mixture, and immediately mixed and aliquoted in 45μL triplicates to a CORNING 384 well black plate. Fluorescence signal was measured in a BioTek Neo 2 Plate reader set at excitation and emission wavelengths of 355 and 450nm, respectively. %Activity was subsequently calculated for each compound concentration against the fluorescence signal of HexA without any compound. GraphPad Prism 2016 was used to calculate IC50 values for each compound.

HEXB: IC50 values for compounds against Recombinant Human Hexosaminidase B (HexB) enzyme, purchased from R&D Systems (cat# 8907-GH-020) were determined by measuring the change in fluorescent signal corresponding to the rate of hydrolytic activity against the commercially available artificial substrate, 4-Methylumbelliferone N-acetyl-β-D-galactosaminide. HexB inhibition assays were performed in a buffer of 100mM MES at pH 5.5 and 5.0nM [HexB], in the presence or absence of various concentrations of compounds and at a fixed substrate concentration of 150μM and 5% DMSO. First, compounds were serially diluted to the desired range

of concentrations in 10% DMSO buffer. Next, 50µL of compound solutions at various concentrations in 10% DMSO Buffer was added to 50µL of 20nM enzyme and allowed to incubate at 25°C for 5 minutes. 100µL of 300µM and 5% DMSO substrate was then added and reaction mixture was immediately mixed and aliquoted in 45µL triplicates to a CORNING 384 well black plate. Fluorescence signal was measured continuously for 20 minutes at 25°C in a BioTek Neo 2 Plate reader set at excitation and emission wavelengths of 355 and 450nm, respectively. Max reaction rates for all compound concentrations were calculated within Gen5 BioTek reader software. %Activity was subsequently calculated for each compound concentration against the max reaction rate of HexB without any compound. GraphPad Prism 2016 was used to calculate the IC50 values for each compound.

NAGZ: IC50 values for compounds against the NagZ enzyme were determined by measuring the change in fluorescent signal corresponding to the rate of hydrolytic activity against the commercially available artificial substrate, 4-Methylumbelliferone N-acetyl-β-D-glucosaminide. NagZ inhibition assays were performed in a buffer of phosphate-buffered saline at pH 7.4 and 2.0nM [NagZ], in the presence or absence of various concentrations of compounds and at a fixed substrate concentration of 60µM and 5% DMSO. First, compounds were serially diluted to the desired range of concentrations in 10% DMSO buffer. Next, 50µL of compound solutions at various concentrations in 10% DMSO Buffer was added to 50µL of 8nM enzyme and allowed to incubate at 25°C for 5 minutes. 100µL of 120µM and 5% DMSO substrate was then added and reaction mixture was immediately mixed and aliquoted in 45µL triplicates to a CORNING 384 well black plate. Fluorescence signal was measured continuously for 20 minutes at 25°C in a BioTek Neo 2 Plate reader set at excitation and emission wavelengths of 355 and 450nm, respectively. Max reaction rates for all compound concentrations were calculated within Gen5 BioTek reader software. %Activity was subsequently calculated for each compound concentration against the max reaction rate of NagZ without any compound. GraphPad Prism 2016 was used to calculate the IC50 values for each compound.

hOGA: IC50 values for compounds against the human Protein O-GlcNAcase (hOGA) enzyme, were determined by measuring the change in fluorescent signal corresponding to the rate of hydrolytic activity against the artificial substrate, Resorufin-N-acetyl-β-D-glucosaminide (synthesized by Sandeep Bhosale of the Vocadlo Lab). hOGA inhibition assays were performed in a buffer of 20mM HEPES, 5mM EDTA, 150mM KCl, pH 7.1 and 0.2nM [hOGA], in the presence or absence of various concentrations of compounds and at a fixed substrate concentration of 25µM and 1% DMSO. First, compounds were serially diluted to the desired range of concentrations in 2% DMSO buffer. Next, 50µL of compound solutions at various concentrations in 2% DMSO Buffer was added to 50µL of 0.8nM enzyme and allowed to incubate at 25°C for 5 minutes. 100µL of 50µM and 1% DMSO substrate was then added and the reaction mixture was immediately mixed and aliquoted in 45µL triplicates to a CORNING 384 well black plate. Fluorescence signal was measured continuously for 20 minutes at 37°C in a BioTek Neo 2 Plate reader set at excitation and emission wavelengths of 572 and 610nm, respectively. Max reaction rates for all compound concentrations were calculated within Gen5 BioTek reader software. %Activity was subsequently calculated for each compound concentration against the max reaction rate of hOGA without any compound. GraphPad Prism 2016 was used to calculate the IC50 values for each compound.

General Procedure A for deprotection by hydrogenolysis: The benzylated compound was dissolved in a mixture THF/*i*-PrOH (0.05 M - 1/1, v/v) then a solution of HCl (1N, 3 eq.), Pd/C (0.5 mass eq.) and black Pd (0.5 mass eq.) were added. The mixture was stirred overnight under H_2 atmosphere, filtrated through a pad of Celite® (previously washed with 1N HCl and water) and concentrated to give the deprotected compound as its hydrochloride salt.

(2*R*,3a*R*,5*R*,6*R*,7*S*,7a*R*)-4-benzyl-6,7-bis(benzyloxy)-5-[(benzyloxy)methyl]-2-(iodomethyl)octa hydrofuro[3,2-b]pyridine **C**

I_2 (3.88 g, 15.29 mmol) was added to a solution of **B** (5.00 g, 7.65 mmol) in anhydrous THF (153 ml) under argon at -20 ° C. The mixture was then stirred at -20 ° C for 24 h. A saturated solution of $Na_2S_2O_3$ (100 mL) was added and the mixture was stirred for 10 min. at rt. The aqueous layer was extracted with Et_2O (3 x 50 mL), the combined organic layers dried over $MgSO_4$ and concentrated. The crude was purified by flash chromatography (RediSep® 80 g, PE / EtOAc 95 : 5 to 90 : 10) to give **C** as a yellow oil (2.48 g, 47%). R*f* = 0.39 (PE/EtOAc 90 : 10); $[\alpha]_D$ = - 13.0 (*c* 1.0, $CHCl_3$); ^{1}H NMR (400 MHz, $CDCl_3$): δ 7.47-7.10 (m, 20H, *CH*-Ar), 5.01 (d, *J* = 11.5 Hz, 1H, OCH*H*-Ph), 4.83 (d, *J* = 11.5 Hz, 1H, OCH*H*-Ph), 4.66 (d, *J* = 11.2 Hz, OCH*H*-Ph), 4.50-4.41 (m, 3H, O*CH*$_2$-Ph), 4.19 (t, *J* = 8.4 Hz, 1H, H-7a), 4.01-3.92 (m, 2H, NCH*H*-Ph, H-2), 3,89 (t, *J* = 8.5 Hz, 1H, H-7), 3.73-3.56 (m, 5H, NCH*H*-Ph, C*H*$_2$-OBn, H-6, H-3a), 3.33 (dd, *J* = 10.0 Hz, *J* = 4.8 Hz, 1H, CH*H*-I), 3.25 (dd, *J*= 10.0 Hz, *J* = 6.7 Hz, 1H, CH*H*-I), 3.03 (q, *J* = 4.6 Hz, 1H, H-5), 2.30-2.24 (m, 1H, H-3), 1.68 (br, q, *J* = 10.5 Hz, 1H, H-3); ^{13}C NMR (100 MHz, $CDCl_3$): δ 139.3, 139.1, 138.6, 138.1 (C^{IV}-Ar), 128.5-127.1 (*CH*-Ar), 84.4 (C-7), 80.9 (C-7a), 80.0 (C-6), 77.8 (C-2), 74.3, 73.4, 73.1 (O*CH*$_2$-Ph), 67.1 (*CH*$_2$-OBn), 61.0 (C-3a), 59.4 (C-5), 54.9 (N*CH*$_2$-Ph), 36.2 (C-3), 10.3 (*CH*$_2$-I); HRMS (ESI$^+$) m/z calcd for $C_{37}H_{41}INO_4$ $[M+H]^+$: 690.2075, found: 690.2107.

(2*S*,3a*R*,5*R*,6*R*,7*S*,7a*S*)-4-benzyl-6,7-bis(benzyloxy)-5-((benzyloxy)methyl)-2-methyloctahydro furo[3,2-b]pyridine **12**

To a solution of **C** (235 mg, 0.34 mmol) in anhydrous THF (40 mL) was added $LiAlH_4$ (52 mg, 1.36 mmol, 4 eq.), then the mixture was stirred at rt for 4 h, neutralized with EtOAc (20 mL) and washed with water H_2O (20 mL). The organic layer was dried over $MgSO_4$, concentrated and the crude was purified by flash chromatography (PE/EtOAc 100 : 0 to 95 : 5) to give **12** (61 mg, 32%) as a colorless oil. R*f* (PE/EtOAc 95 : 5); $[\alpha]_D$ = + 11.0 (c 1.0, $CHCl_3$); ^{1}H NMR (400 MHz, $CDCl_3$): δ 7.45-7.19 (m, 20H, *CH*-Ar), 5.01 (d, *J* = 11.6 Hz, 1H, O*CH*H-Ph), 4.82 (d, *J* = 11.6 Hz, 1H, O*CH*H-Ph), 4.61 (d, *J* = 11.2 Hz, 1H, O*CH*H-Ph), 4.49-4.43 (m, 3H, O*CH*$_2$-Ph), 4.08-4.00 (m, 2H, H-7a, H-2), 3.96 (d, *J* = 14.0 Hz, 1H, N*CH*H-Ph), 3.88 (t, *J* = 8.4 Hz, 1H, H-7), 3.70-3.63 (m, 3H, N*CH*H-Ph, *CH*H-OBn, H-3a), 3.63-3.57 (m, 2H, *CH*H-OBn, H-6), 3.06 (like dd, *J* = 9.2 Hz, *J* = 4.6 Hz, 1H, H-5), 2.19-2.13 (m, 1H, H-3), 1.52 (like dd, *J* = 22.0 Hz, J = 10.9 Hz, 1H, H-3), 1.33 (d, *J* = 6.0 Hz, 3H, CH_3); ^{13}C NMR (100 MHz, $CDCl_3$): δ 139.5, 138.7, 138.2 (C^{IV}-Ar), 128.5-127.0 (*CH*-Ar), 84.8 (C-7), 80.4 (C-6) 80.0 (C-7a), 74.6 (C-2), 74.2, 73.4, 72.7 (O*CH*$_2$-Ph), 67.2 (*CH*$_2$-OBn), 61.4 (C-3a), 59.6 (C-5), 55.0 (N*CH*$_2$-Ph), 38.6 (C-3), 21.6 (CH_3); HRMS (ESI$^+$) m/z calcd for $C_{37}H_{42}NO_4$ $[M+H]^+$: 564.3114, found: 564.3110.

((2*R*,3a*R*,5*R*,6*R*,7*S*,7a*S*)-4-benzyl-6,7-bis(benzyloxy)-5-((benzyloxy)methyl)octahydrofuro[3,2-b]pyridin-2-yl)methyl acetate **13**

AgOAc (242 mg, 1.45 mmol) was added to a solution of **C** (100 mg, 0.145 mmol) in dry toluene (2.2 mL) at rt under argon, then the mixture was stirred at 50° C for 48 h. After filtration through a pad of Celite® and concentration, the crude was purified by flash chromatography (PE/EtOAc 80:20) to give **13** (55 mg, 61%) as a colorless oil. R*f* = 0.16 (PE/EtOAc 85 : 15); $[\alpha]_D$ = + 5.1 (*c* 1.0, $CHCl_3$); ^{1}H NMR (400 MHz, $CDCl_3$) δ 7.35-7,28 (m, 20H, *CH*-Ar), 4.96 (d, *J* = 11.5 Hz, 1H, O*CH*H-Ph), 4.80 (d, *J* = 11.5 Hz, 1H, O*CH*H-Ph), 4.66 (d, *J* = 11.5 Hz, 1H, O*CH*H-Ph), 4.49-4.45 (m, 3H, O*CH*$_2$-Ph), 4.26 (dd, *J* = 3.4 Hz, *J* = 11.4, 1H, CH*H*-OAc), 4.15-4.08 (m, 3H, H-2, H-7a, C*H*H-OAc), 4.00 (d, *J* = 13.7 Hz, 1H, N*CH*H-Ph), 3.82 (t, $J_{H\text{-}7/H\text{-}7a}$ = 8.4 Hz, 1H, H-7), 3.70-3.59 (m, 5H, N*CH*H-Ph, *CH*$_2$-OBn, H-6, H-3a), 3.05 (q, *J* = 4.7 Hz, 1H, H-5), 2.11 (m, 4H, CH_3, H-3), 1.70 (q, *J* = 10.9 Hz, 1H, H-3); ^{13}C NMR (100 MHz, $CDCl_3$) δ 170.9 (C=O), δ 139.1, 139.1, 138.4, 137.9 (C^{IV}-Ar), 128.3-127.0 (*CH*-Ar), 84.2 (C-7), 80.1 (C-7a), 79.8 (C-6), 76.0 (C-2), 73.9, 73.3, 72.9 (O*CH*$_2$-Ph), 67.0 (*CH*$_2$-OBn), 66.4 (*CH*$_2$-OAc), 60.5 (C-3a), 59.4 (C-5), 54.9 (N*CH*$_2$-Ph), 31.5 (C-3), 20.9 (CH_3); HRMS (ESI$^+$) m/z calcd for $C_{39}H_{44}NO_6$ $[M+H]^+$: 622.3178, found: 622.3163.

(2R,3aR,5R,6R,7S,7aS)-2-(azidomethyl)-4-benzyl-6,7-bis(benzyloxy)-5-((benzyloxy)methyl)octa hydrofuro[3,2-b]pyridine **14**

NaN_3 (57 mg, 0.88 mmol) was added to a solution of **C** (300 mg, 0.43 mmol) in dry DMF (5.5 mL), then the mixture was stirred under Ar at rt for 27 h. After concentration, the crude was purified by flash chromatography (RediSep® 4 g, PE / EtOAc 95 : 5 to 85 : 15) to give **14** as a yellow oil (115 mg, 40%). R*f* = 0.35 (PE/EtOAc 85 : 15); $[\alpha]_D$ = - 17.3 (c 1.0, $CHCl_3$); ^{1}H NMR (400 MHz, $CDCl_3$) δ 7.40-7.17 (m, 20H, *CH*-Ar), 4.96 (d, *J* = 11.4 Hz, 1H, OC*H*H-Ph), 4.79 (d, *J* = 11.4 Hz, 1H, OC*H*H-Ph), 4.61 (d, *J* = 11.2 Hz, 1H, OC*H*H-Ph), 4.46-4.44 (m, 3H, OCH_2-Ph), 4.11 (t, $J_{H\text{-}7a/H\text{-}7}$ = 8.4 Hz, 1H, H-7a), 4.09-4.05 (m, 1H, H-2), 3.95 (d, *J* = 13.9 Hz, 1H, NC*H*H-Ph), 3.88 (t, $J_{H\text{-}7/H\text{-}7a}$ = 8.4 Hz, 1H, H-7), 3.69-3.58 (m, 5H, NC*H*H-Ph, CH_2-OBn, H-6, H-3a), 3.42 (dd, *J* = 12.9 Hz, *J* = 3.8 Hz, 1H, *CH*H-N_3), 3.33 (dd, *J* = 12.9 Hz, *J* = 5.5 Hz, 1H, *CH*H-N_3), 3.03 (q, *J* = 4.6 Hz, 1H, H-5), 2.06 (ddd, *J* = 10.5 Hz, *J* = 6.7 Hz, *J* = 5.2 Hz, 1H, H-3), 1.75 (q, *J* = 10.9 Hz, 1H, H-3); ^{13}C NMR (100 MHz, $CDCl_3$) δ 139.3, 139.2, 138.5, 138.1 (C^{IV}-Ar), 128.5-127.2 (*CH*-Ar), 84.5 (C-7), 80.5 (C-7a), 80.0 (C-6), 77.3 (C-2), 74.3, 73.5, 73.0 (OCH_2-Ph), 67.1 (CH_2-OBn), 60.8 (C-3a), 59.4 (C-5), 54.9 (NCH_2-Ph), 54.7 (CH_2-N_3), 33.1 (C-3); HRMS (ESI^+) m/z calcd for $C_{37}H_{41}N_4O_4$ $[M+H]^+$: 605.3122, found: 605.3149.

N-(((2*R*,3a*R*,5*R*,6*R*,7*S*,7a*S*)-4-benzyl-6,7-bis(benzyloxy)-5-((benzyloxy)methyl)octahydrofuro[3,2-b]pyridin-2-yl)methyl)acetamide **15**

To a solution of **14** (60 mg, 0.099 mmol) in a mixture THF/NH_4OH (3 mL / 0.3 mL), at rt, was added triphenylphosphine polymer bound (153 mg, 3.2 mmol/g, 0.49 mmol). The mixture was stirred at 50 °C for 5 h, filtrated through a pad of Celite® and concentrated. The crude was taken up in Ac_2O/Pyridine (0.7 mL/0.7 mL) and stirred at rt overnight, then concentrated and co-evaporated twice with toluene. The crude was purified by flash chromatography (PE / EtOAc 85 : 15) to give **15** (32 mg, 52%) as a yellow oil. R*f* = 0.35 (PE/EtOAc 85 : 15); $[\alpha]_D$ = - 70.2 (c 1,0, $CHCl_3$); ^{1}H NMR (400 MHz, $CDCl_3$) δ 7.37-7.30 (m, 20H, *CH*-Ar), δ 5.68 (t, 1H, N-H), 4.86 (s, 2H, OCH_2-Ph), 4.58 (d, *J* = 11.2 Hz, 1H, OC*H*H-Ph), 4.48-4.45 (m, 3H, OC*H*H-Ph, OCH_2-Ph), 4.06 (t, *J* = 8.1 Hz, 1H, H-7a), 3.99-3.92 (m, 2H, NCH*H*-Ph, H-2), 3.78 (t, $J_{H\text{-}7/H\text{-}7a}$ = 7.5 Hz, 1H, H-7), 3.68-3.54 (m, 6H, NC*H*H-Ph, CH_2-OBn, H-6, H-3a, CH*H*-NHAc), 3.17 (m, 1H, C*H*H-NHAc), 3.05 (q, *J* = 4.7 Hz, 1H, H-5), 2.10 (m, 1H, H-3), 1.87 (s, 3H, CH_3), 1.58 (q, *J* = 10.4 Hz, H-3); ^{13}C NMR (100 MHz, $CDCl_3$) δ 170.3 (C=O), δ 139.4, 139.2, 139.0, 138.9 (C^{IV}-Ar), 129.1-127.0 (*CH*-Ar), 82.9 (C-7), 80.1 (C-6), 79.3 (C-7a), 77.1 (C-2), 73.4, 73.4, 72.5 (OCH_2-Ph), 66.6 (CH_2-OBn), 60.4 (C-3a), 59.1 (C-5), 54.7 (NCH_2-Ph), 43.2 (CH_2NHAc) , 33.1 (C-3), 23.2 (CH_3); HRMS (ESI^+) m/z calcd for $C_{39}H_{44}N_2O_5$ $[M+H]^+$: 621.3346, found: 621.3322.

(2*R*,3a*R*,5*R*,6*R*,7*S*,7a*S*)-4-benzyl-6,7-bis(benzyloxy)-5-((benzyloxy)methyl)-2-((4-heptyl-1H-1,2,3-triazol-1-yl)methyl)octahydrofuro[3,2-b]pyridine **16**

To a solution of 14 (35 mg, 57.8 ⊚mol) in anhydrous CH_2Cl_2 (1 mL), at rt under Ar, were added lutidine (7.0 ⊚L, 1 eq.), nonyne (11.4 ⊚L, 69.4 ⊚mol) and tetrakis(acetonitrile) copper(I) hexafluorophosphate complex (10.8 mg, 28.9 ⊚mol). The mixture was stirred for 2h at rt, then diluted with CH_2Cl_2 and washed with a solution of Na_2EDTA (2M). The organic layer was dried over $MgSO_4$, filtrated and concentrated. The crude was purified by flash chromatography (PE/EtOAc 70/30) to give **16** (21 mg, 50 %) as a colorless oil. R*f* (EP/AcOEt 60:40) = 0.41; $[\alpha]_D$ = - 12,5 (c 1.0, $CHCl_3$); ^{1}H NMR (500 MHz, $CDCl_3$): δ 7.32-7.10 (m, 21H, 20*CH*-Ar, *CH*-triazol), 4.75 (d, *J* = 6.4 Hz, 2H, OCH_2-Ph), 4.46 (m, 2H, OC*H*H-Ph, *CH*H-N-triazol), 4.34 (m, 3H, OC*H*H-Ph,), 4.26 (dd, *J* = 6.7 Hz, *J* = 14.1 Hz, 1H, *CH*H-N-triazol), 4.11 (m, 1H, H-2), 4.02 (t, *J* = 8.2 Hz, 1H, H-7a), 3.80 (d, *J* = 13.8 Hz, 1H, NC*H*H-Ph), 3.68 (t, *J*= 7.8 Hz, 1H, H-7), 3.53 (m, 5H, NC*H*H-Ph, CH_2-OBn, H-6, H-3a), 2.92 (m, 1H, H-5), 2.57 (t, *J* = 7.8 Hz, 2H, CH_2-triazol), 2.10 (m, 1H, H-3), 1.52 (m, 3H, CH_2-chain, H-3), 1.22 (m, 8H, CH_2-chain), 0.79 (t, *J* = 7.0 Hz, 3H, CH_3); ^{13}C NMR (125 MHz, $CDCl_3$): δ 148.4 (C-triazol), 138.9, 138.7, 138.2, 137.9 (C^{IV}-Ar), 128.4-127.1 (*CH*-Ar), 121.8 (CH-triazol), 83.5 (C-7), 80.1 (C-7a), 79.9 (C-6), 76.7 (C-2), 73.9, 73.2, 72.3 (OCH_2-Ph), 66.5 (CH_2-OBn), 60.2 (C-3a), 59.1 (C-5), 54.6 (NCH_2-Ph), 53.8 (CH_2-Ntriazol), 33.4 (C-3), 31.7, 29.5, 29.3, 29.0, 25.7, 22.6 (CH_2-chain), 14.1 (CH_3); HRMS (ESI^+) m/z calcd for $C_{46}H_{56}N_4NaO_4$ $[M+Na]^+$: 751.4194, found: 751.4200.

(2*R*,3a*R*,5*R*,6*R*,7*S*,7a*S*)-4-benzyl-6,7-bis(benzyloxy)-5-((benzyloxy)methyl)-2-((4-(4-phenylbutyl)-1H-1,2,3-triazol-1-yl)methyl)octahydrofuro[3,2-b]pyridine **17**

To a solution of **14** (60 mg, 0.099 mmol) in anhydrous CH_2Cl_2 (2 mL), at rt under Ar, were added lutidine (6 µL, 0.049 mmol), 5-phenylpentyne (18 µL, 0.12 mmol) and tetrakis(acetonitrile) copper(I) hexafluorophosphate complex (18.5 mg, 0.049 mmol). The mixture was stirred for 4h at rt, then diluted with CH_2Cl_2 and washed with a solution of Na_2EDTA (2M). The organic layer was dried over $MgSO_4$, filtrated and concentrated. The crude was purified by flash chromatography (PE/EtOAc 60/40) to give **17** (40 mg, 54 %) as a colorless oil. R*f* (EP/AcOEt 60:40) = 0.25; $[\alpha]_D$= - 19.0 (c 1.0, $CHCl_3$); ^{1}H NMR (500 MHz, $CDCl_3$): δ 7.27-7.07 (m, 21H, 20C*H*-Ar, C*H*-triazol), 4.72 (s, 2H, OC*H*$_2$-Ph), 4.48 (m, 1H, C*H*H-N-triazol), 4.42 (d, 1H, *J* = 11.2 Hz, OC*H*H-Ph), 4.34 (m, 4H, C*H*H-N-triazol, 3xOC*H*H-Ph), 4.11 (m, 1H, H-2), 4.01 (t, 1H, *J* = 8.0 Hz, H-7a), 3.79 (d, 1H, *J* = 13.9 Hz, NC*H*H-Ph), 3.68 (t, 1H, *J* = 7.6 Hz, H-7), 3.59-3.47 (m, 5H, NC*H*H-Ph, C*H*$_2$-OBn, H-6, H-3a), 2.94 (m, 1H, H-5), 2.58 (m, 4H, C*H*$_2$-chain), 2.12 (m, 1H, H-3), 1.89 (brs, 2H, C*H*$_2$-chain), 1.50 (m, 1H, H-3); ^{13}C NMR (125 MHz, $CDCl_3$): δ 141.7 (C-triazol), 138.8, 138.6, 138.2, 137.9 (C^{IV}-Ar), 128.5-127.1 (*C*H-Ar), 125.8 (*C*H-triazol), 83.1 (C-7), 80.1 (C-7a), 79.8 (C-6), 76.5 (C-2), 73.3, 73.3, 72.3 (O*C*H$_2$-Ph), 66.5 (*C*H$_2$-OBn), 60.1 (C-3a), 59.0 (C-5), 54.6 (N*C*H$_2$-Ph), 54.2 (*C*H$_2$-N-triazol), 35.4 (2x*C*H$_2$-chain), 34.5 (C-3), 31.0 (*C*H$_2$-chain); HRMS (ESI$^+$) m/z calcd for $C_{48}H_{52}N_4NaO_4$ [M+Na]$^+$: 771.3881, found: 771.3884.

N-(((2*R*,3a*R*,5*R*,6*R*,7*S*,7a*S*)-4-benzyl-6,7-bis(benzyloxy)-5-((benzyloxy)methyl)octahydrofuro[3,2-b]pyridin-2-yl)methyl)nonanamide **18**

To a solution of **14** (78 mg, 0.13 mmol) in a mixture THF/NH_4OH (3 mL / 0.3 mL), at rt, was added triphenylphosphine polymer bound (122 mg, 3.2 mmol/g, 0.39 mmol). The mixture was stirred at 50 °C for 15 h, filtrated through a pad of Celite® and concentrated to give the expected amino derivative. To a solution of the crude in dry CH_2Cl_2 (2.4 mL), at 0°C under argon, were added triethylamine (54 µL, 0.39 mmol) and nonanoyl chloride (46 µL, 0.26 mmol). The mixture was stirred at 0°C for 1h30, diluted with CH_2Cl_2 and washed with 1N HCl and brine. The organic layer was dried over $MgSO_4$, filtrated and concentrated. The crude was purified by flash chromatography (PE/EtOAc 70/30 then 60/40) to give **18** (45 mg, 48 %, 2 steps) as a colorless oil. R*f* (EP/AcOEt 60:40) = 0.33; $[\alpha]_D$ = + 21.2 (c 1.0, $CHCl_3$); ^{1}H NMR (500 MHz, $CDCl_3$): δ 7.33-7.10 (m, 20H, C*H*-Ar), 4.72 (s, 2H, OC*H*$_2$-Ph), 5.45 (t, 1H, *J* = 5.7 Hz, NH), 4.77 (s, 2H, OC*H*$_2$-Ph), 4.48 (d, 1H, *J* = 11.2 Hz, OC*H*H-Ph), 4.36 (m, 3H, 3xOC*H*H-Ph), 3.95 (t, 1H, *J* = 8.3 Hz, H-7a), 3.83 (m, 2H, H-2, NC*H*H-Ph), 3.65 (t, 1H, *J* = 8.4 Hz, H-7), 3.57-3.47 (m, 5H, NC*H*H-Ph, *C*H$_2$-OBn, H-6, H-3a), 3.45 (m, 1H, *CH*H-NHCO), 3.08 (m, 1H, *CH*H-NHCO), 2.90 (dd, 1H, *J* = 4.6 Hz, *J* = 9.1 Hz, H-5), 1.96 (m, 3H, H-3, *C*H$_2$-chain), 1.45 (m, 3H, H-3, *C*H$_2$-chain), 1.19 (m, 10H, 5x*C*H$_2$-chain), 0.80 (t, 3H, *J* = 6.9 Hz, *C*H$_3$); ^{13}C NMR (125 MHz, $CDCl_3$): δ 173.2 (C=O), 139.2, 138.8, 138.3, 137.9 (C^{IV}-Ar), 128.4-127.0 (*C*H-Ar), 83.3 (C-7), 80.2 (C-6), 79.2 (C-7a), 77.2 (C-2), 73.3, 73.3, 72.5 (O*C*H$_2$-Ph), 66.5 (*C*H$_2$-OBn), 60.5 (C-3a), 59.1 (C-5), 54.6 (N*C*H$_2$-Ph), 42.8 (*C*H$_2$-NHCO), 36.7 (*C*H$_2$-chain), 32.8 (C-3), 31.8, 29.3, 29.2, 29.1, 25.8, 22.6 (6 x *C*H$_2$-chain), 14.1 (*C*H$_3$); HRMS (ESI$^+$) m/z calcd for $C_{46}H_{59}N_2O_5$ [M+H]$^+$: 719.4418, found: 719.44.22.

(2*S*,3a*R*,5*R*,6*R*,7*S*,7a*S*)-5-(hydroxymethyl)-2-methyloctahydrofuro[3,2-b]pyridine-6,7-diol hydrochloride **5**

The general procedure A was applied to compound **12** (20 mg, 27.4 µmol) to give compound **5** (24 mg, 99%) as a colorless oil. $[\alpha]_D$ = + 45.0 (c 0.5, MeOH); ^{1}H NMR (400 MHz, methanol-d4): δ 4.15 (m, 1H, H-3a), 4.06 (m, 1H, H-2), 3.97-3.89 (m, 3H, C*H*$_2$-OBn, H-7a), 3.79 (like t, *J* = 7.8, 6.1 Hz, 1H, H-7), 3.66 (t, *J* = 8.0 Hz, 1H, H-6), 3.28 (m, 1H, H-5), 2.57 (m, 1H, H-3), 1.71 (m, 1H, H-3), 1.42 (d, *J* = 5.4 Hz, 3H, CH_3); ^{13}C NMR (100 MHz, methanol-d4): δ 80.8 (C-7a), 76.1 (C-2), 73.5 (C-7), 67.7 (C-6), 59.5 (C-5), 59.2 (*C*H$_2$OBn), 55.5 (C-3a), 37.6 (C-3), 20.8 (*C*H$_3$); HRMS (ESI$^+$) m/z calcd for $C_9H_{18}NO_4$ [M+H]$^+$: 204.1236, found: 204.1233.

(2*R*,3a*R*,5*R*,6*R*,7*S*,7a*S*)-2,5-bis(hydroxymethyl)octahydrofuro[3,2-b]pyridine-6,7-diol hydrochloride **6**

MeONa (0.4 mg, $4.5.10^{-6}$ mol) was added to a solution of **13** (28 mg, $4.5.10^{-5}$ mol) in dry methanol (1 mL) at 0 ° C under Ar. The mixture was stirred at rt overnight, then neutralized with acidic Amberlyst, filtrated and concentrated to give the expected deacetylated compound. The crude (18 mg, $3.1.10^{-5}$ mol) was directly submitted to the general procedure A to give **6** (9 mg, 72%, 2 steps) as a colorless oil. $[\alpha]_D$ = + 70.7 (c 1.0, H_2O); ^{1}H NMR (500 MHz, d_2O): δ 4.22 (m, 1H, H-2), 4.17 (dd, *J* = 4.3 Hz, *J* = 12.4 Hz, 1H, H-3a), 4.01 (t, *J* = 8.4 Hz, 1H, H-7a), 3.94 (dd, *J* = 4.3 Hz, *J* = 12.4 Hz, 1H, C5-*CH*$_2$-OH), 3.84 (dd, *J* = 4.3 Hz, *J* = 12.4 Hz, 1H, C5-*CH*$_2$-OH), 3.78 (m, 2H, H-7, C2-*CH*$_2$-OH), 3.66 (t, *J* = 8.4 Hz, 1H, H-6), 3.58 (dd, *J* = 4.3 Hz, *J* = 12.4 Hz, 1H, C2-*CH*$_2$-OH), 3.39 (m, 1H, H-5), 2.42 (m, 1H, H-3), 2.02 (m, 1H, H-3); ^{13}C NMR (125 MHz, d_2O): δ 78.8 (C-2), 78.5 (C-7a), 71.5 (C-7), 65.8 (C-6), 62.2 (C2-*CH*$_2$-OH), 57.0 (C5-*CH*$_2$-OH), 56.9 (C-5), 52.6 (C-3a), 28.9 (C-3); HRMS (ESI$^+$) m/z calcd for $C_9H_{18}NO_5$ $[M+H]^+$: 220.1179, found: 220.1180.

(2*R*,3a*R*,5*R*,6*R*,7*S*,7a*S*)-2-(aminomethyl)-5-(hydroxymethyl)octahydrofuro[3,2-b]pyridine-6,7-diol dihydrochloride **7**

The general Procedure A was applied to compound **14** (35 mg, 0.06 mmol) to give compound **7** (17 mg, 99%) as a brown oil. $[\alpha]_D$ = - 8.4 (c 2.5, MeOH); ^{1}H NMR (400 MHz, methanol-d4): δ 4.26-4.19 (m, 2H, H-3a, H-2), 4.04 (t, *J* = 6.2 Hz, 1H, H-7a), 3.96-3.90 (m, 2H, *CH*$_2$-OH), 3.86-3.82 (m, 1H, H-7), 3.68 (t, *J* = 7.9 Hz, 1H, H-6), 3.37-3.32 (m, 2H, H-5, *CH*H-NH$_2$), 3.19 (dd, *J* = 12.9 Hz, *J* = 9.8 Hz, 1H, *CH*H-NH$_2$), 2.68-2.61 (m, 1H, H-3), 2.01-1.93 (m, 1H, H-3); ^{13}C NMR (100 MHz, methanol-d4): δ 81.1 (C-7a), 76.1 (C-2), 73.0 (C-7), 67.8 (C-6), 59.1 (*CH*$_2$-OH, C-5), 54.9 (C-3a), 44.3 (*CH*$_2$-NH$_2$), 33.2 (C-3); HRMS (ESI$^+$) m/z calcd for $C_9H_{19}N_2O_4$ $[M+H]^+$: 219.1339, found: 219.1341.

N-(((2R,3aR,5R,6R,7S,7aS)-6,7-dihydroxy-5-(hydroxymethyl)octahydrofuro[3,2-b]pyridin-2-yl) methyl)acetamide hydrochloride **8**

The general procedure A was applied to compound **15** (32 mg, $5.2.10^{-5}$ mol) to give **8** (14 mg, 94 %) as a yellow foam. $[\alpha]_D$ = + 24.0 (c 1.0, MeOH); ^{1}H NMR (500 MHz, methanol-d4): δ 4.18 (m, 1H, H-3a), 4.07 (m, 1H, H-2), 3.95 (t, *J* = 6.3 Hz, 1H, H-7a), 3.90 (m, 2H, *CH*$_2$-OH), 3.78 (dd, *J* = 6.4 Hz, *J* = 8.1 Hz, 1H, H-7), 3.61 (m, 2H, H-6, *CH*H-NHAc), 3.48 (dd, *J* = 6.8 Hz, *J* = 14.1 Hz, 1H, *CH*H-NHAc), 3.31 (m, 1H, H-5), 2.50 (m, 1H, H-3), 2.11 (s, 1H, *CH*$_3$), 1.85 (m, 1H, H-3); ^{13}C NMR (125 MHz, methanol-d4): δ 174.8 (C=O), 80.9 (C-7a), 78.2 (C-2), 73.4 (C-7), 67.8 (C-6), 59.23 (C-5), 59.19 (*CH*$_2$-OH), 55.1 (C-3a), 44.4 (*C*H$_2$-NHAc), 33.0 (C-3), 21.8 (*CH*$_3$); HRMS (ESI$^+$) m/z calcd for $C_{11}H_{21}N_2O_5$ $[M+H]^+$: 261.1445, found: 261.1444.

(2R,3aR,5R,6R,7S,7aS)-2-((4-heptyl-1H-1,2,3-triazol-1-yl)methyl)-5-(hydroxymethyl)octa-hydrofuro [3,2-b]pyridine-6,7-diol hydrochloride **9**

The general procedure A was applied to compound **16** (20 mg, 27.4 ⊚mol) to give **9** (12 mg, quant.) as a colorless oil. R*f* (AcOEt/MeOH 70:30) = 0.26; $[\alpha]_D$ = - 19.0 (c 1.0, MeOH); ^{1}H NMR (500 MHz, methanol-d4): δ 8.43 (s, 1H, *CH*-triazol), 4.97 (m, 1H, *CH*H-N-triazol), 4.81 (dd, *J* = 8.2 Hz, *J* = 14.2 Hz, 1H, *CH*H-N-triazol), 4.43 (m, 1H, H-2), 4.23 (m, 1H, H-3a), 3.99 (t, *J* = 6.4 Hz, 1H, H-7a), 3.93 (dd, *J* = 5.9 Hz, *J* = 12.0 Hz, 1H, *CH*H-OH), 3.87 (dd, *J* = 3.4 Hz, *J* = 11.9 Hz, 1H, *CH*H-OH), 3.74 (dd, *J* = 6.3 Hz, *J* = 8.0 Hz, 1H, H-7), 3.63 (t, *J* = 8.2 Hz, 1H, H-6), 3.26 (m, 1H, H-5), 2.85 (t, *J* = 7.7 Hz, 2H, *CH*$_2$-Ctriazol), 2.67 (m, 1H, H-3), 2.03 (m, 1H, H-3), 1.75 (m, 2H, C*H*$_2$-chain), 1.36 (m, 8H, C*H*$_2$-chain), 0.91 (t, *J* = 6.8 Hz, 3H, *CH*$_3$); ^{13}C NMR (125 MHz, methanol-d4): δ 146.6 (C-triazol), 128.0 (*C*H-triazol), 81.3 (C-7a), 77.4 (C-2), 73.3 (C-7), 67.7 (C-6), 59.05 (C-5), 59.02 (*CH*$_2$-OH), 56.5 (*C*H$_2$-N-triazol), 54.6 (C-3a), 32.8 (*CH*$_2$-chain), 32.7 (C-3), 30.1, 30.0, 29.5, 29.0, 24.7, 23.7 (*CH*$_2$-chain), 14.4 (*CH*$_3$); HRMS (ESI$^+$) m/z calcd for $C_{18}H_{33}N_4O_4$ $[M+H]^+$: 369.2496, found: 369.2503.

(2*R*,3a*R*,5*R*,6*R*,7*S*,7a*S*)-5-(hydroxymethyl)-2-((4-(4-phenylbutyl)-1H-1,2,3-triazol-1-yl)methyl) octahydrofuro[3,2-b]pyridine-6,7-diol hydrochloride **10**

The general procedure A was applied to compound **17** (30 mg, 40 ⍵mol) to give **10** (14 mg, 82%) as a colorless oil. R*f* (AcOEt/MeOH 70:30) = 0.30; $[\alpha]_D$ = - 7.7 (c 1.0, MeOH); ^{1}H NMR (500 MHz, methanol-d4): δ 7.87 (s, 1H, *CH*-triazol), 7.25-7.14 (m, 5H, 5*CH*-Ar), 4.72 (m, 1H, *CH*H-N-triazol), 4.60 (m, 1H, *CH*H-N-triazol), 4.33 (brs, 1H, H-2), 4.16 (brs, 1H, H-3a), 3.95 (s, 1H, H-7a), 3.86 (m, 2H, CH_2-OH), 3.61 (m, 2H, H-6, H-7), 3.26 (brs, 1H, H-5), 2.68 (m, 4H, CH_2-chain), 2.55 (brs, 1H, H-3), 1.98 (brs, 3H, CH_2-chain, H-3); ^{13}C NMR (125 MHz, methanol-d4): δ 149.0 (C^{IV}-Ar), 143.1 (C-triazol), 129.5, 129.4, 126.9 (*CH*-Ar), 124.8 (*C*H-triazol), 81.1 (C-7a), 78.2 (C-2), 73.5 (C-7 or C-6), 67.9 (C-6 or C-7), 59.0 (CH_2-OH), 58.7 (C-5), 54.7 (C-3a), 54.2 (*C*H$_2$-N-triazol), 36.3 (CH_2-chain), 32.7 (C-3), 32.3, 25.8 (CH_2-chain); HRMS (ESI$^+$) m/z calcd for $C_{20}H_{29}N_4O_4$ $[M+H]^+$: 389.2183, found: 389.2182.

N-(((2*R*,3a*R*,5*R*,6*R*,7*S*,7a*S*)-6,7-dihydroxy-5-(hydroxymethyl)octahydrofuro[3,2-b]pyridin-2-yl) methyl)nonanamide hydrochloride **11**

The general procedure A was applied to compound **18** (43 mg, 60.0 ⍵mol) to give **11** (23 mg, 97%) as a colorless oil. R*f* (AcOEt/MeOH 70:30) = 0.22; $[\alpha]_D$ = + 13.9 (c 1.0, MeOH); ^{1}H NMR (500 MHz, methanol-d4): δ 4.15 (m, 1H, H-3a), 4.04 (m, 1H, H-2), 3.92 (m, 1H, H-7a), 3.86 (m, 2H, CH_2OH), 3.76 (dd, *J* = 6.6 Hz, *J* = 7.7 Hz, 1H, H-7), 3.62 (t, *J* = 8.3 Hz, 1H, H-6), 3.53 (dd, *J* = 4.0 Hz, *J* = 14.0 Hz, 1H, *CH*NHCO), 3.44 (dd, *J* = 6.6 Hz, *J* = 14.0 Hz, 1H, *CH*NHCO), 3.27 (m, 1H, H-5), 2.48 (m, 1H, H-3), 2.25 (t, *J* = 7.5 Hz, 2H, COCH_2-chain), 1.83 (m, 1H, H-3), 1.61 (t, *J* = 6.9 Hz, 2H, CH_2-chain), 1.31 (m, 10H, CH_2-chain), 0.89 (t, *J* = 6.7 Hz, 3H, CH_3); ^{13}C NMR (125 MHz, methanol-d4): δ 177.0 (C=O), 80.8 (C-7a), 78.6 (C-2), 73.5 (C-7), 67.9 (C-6), 59.2 (CH_2-OH), 59.0 (C-5), 55.1 (C-3a), 43.9 (CONHCH_2-chain), 36.9 (COCH_2-chain), 33.0 (C-3), 30.4, 30.3, 30.3, 27.0, 23.2 (CH_2-chain), 14.5 (CH_3); HRMS (ESI$^+$) m/z calcd for $C_{18}H_{35}N_2O_5$ $[M+H]^+$: 359.2540, found: 359.2540.

Supplementary Materials: Copies of ^{1}H and ^{13}C NMR spectra of compounds **5**-**18**; Conformational analysis of compounds **9** and **11**.

Author Contributions: "Conceptualization, J.D. and Y.B.; synthesis and characterization of compounds, Q.F., J.D. and G.G.; conformational analysis, A.P. and J.J.B.; glycosidase inhibition assays, Y.S., M.K. and A.K.; hexosaminidase assays, C.P., R.A. and D.V.; writing—original draft preparation, J.D. and Y.B.; writing—review and editing, J.D., A.K., D.V. and Y.B.; All authors have read and agreed to the published version of the manuscript."

Funding: This research was funded by a Multi-Investigator Research Initiative co-funded by Brain Canada, the Pacific Alzheimer Research Foundation (PARF), and the Michael Smith Foundation for Health Research (MSFHR) as well as by an operating grant from the Canadian Institutes of Health Research (CIHR, MOP-123341). &DJV is supported as a Tier I Canada Research Chair (CRC) in Chemical Glycobiology.

Acknowledgments: YB acknowledges financial support from the European Union (ERDF) and "Région Nouvelle Aquitaine".

Conflicts of Interest: "The authors declare no conflict of interest."

References

1. A. Varki, R. D. Cummings, J. D. Esko, H. H. Freeze, P. Stanley, C. R. Bertozzi, G. W. Hart and M. E. Etzler, Eds., *Essentials of Glycobiology*, Cold Spring Harbor Laboratory Press, Cold Spring Harbor (NY), 2nd edn., 2009.
2. Cheng, Q.; Li, H.; Merdek, K.; Park, J. T. Molecular Characterization of the β-*N*-Acetylglucosaminidase of *Escherichia coli* and Its Role in Cell Wall Recycling. *J. Bacteriol.*, **2000**, *182*, 4836–4840.
3. King, S. J.; Hippe K. R.; Weiser, J. N. Deglycosylation of human glycoconjugates by the sequential activities of exoglycosidases expressed by Streptococcus pneumoniae. *Mol. Microbiol.*, **2006**, *59*, 961–974.
4. Macauley M. S.; Vocadlo, D. J. Increasing *O*-GlcNAc levels: An overview of small-molecule inhibitors of *O*-GlcNAcase. *Biochimica et Biophysica Acta (BBA) - General Subjects*, **2010**, *1800*, 107–121.
5. Liu, J.; Numa, M. M. D.; Liu, H.; Huang, S.-J.; Sears, P.; Shikhman A. R.; Wong, C.-H. Synthesis and High-Throughput Screening of *N*-Acetyl-β-hexosaminidase Inhibitor Libraries Targeting Osteoarthritis. *J. Org. Chem.*, 2004, **69**, 6273–6283.
6. Reese, T. A.; Liang, H.-E.; Tager, A. M.; Luster, A. D.; Van Rooijen, N.; Voehringer D.; Locksley, R. M. Chitin induces accumulation in tissue of innate immune cells associated with allergy**.** *Nature*, **2007**, *447*, 92–96.
7. Liu, F.; Iqbal, K.; Grundke-Iqbal, I.; Hart G. W.; Gong, C.-X. O-GlcNAcylation regulates phosphorylation of tau: A mechanism involved in Alzheimer's disease. *Proc. Natl. Acad. Sci. U.S.A.*, **2004**, *101*, 10804–10809.
8. Kolter T.; Sandhoff K. Sphingolipids - Their Metabolic Pathways and the Pathobiochemistry of Neurodegenerative Diseases. *Angewandte Chemie International Edition*, **1999**, *38*, 1532–1568.
9. Tropak, M. B.; Blanchard, J. E.; Withers, S. G.; Brown E. D.; Mahuran, D. High-throughput screening for novel human lysosomal β-N-acetyl hexosaminidase inhibitors acting as pharmacological chaperones. *Chem. Biol.*, **2007**, *14*, 153–164.
10. Niedbala, M. J.; Madiyalakan, R.; Matta, K.; Crickard, K.; Sharma M.; Bernacki, R. J. Role of Glycosidases in Human Ovarian Carcinoma Cell Mediated Degradation of Subendothelial Extracellular Matrix. *Cancer Res.*, **1987**, *47*, 4634–4641.
11. (a) Litzinger, S.; Fischer, S.; Polzer, P.; Diederichs, K.; Welte W.; Mayer, C. Structural and Kinetic Analysis of *Bacillus subtilis N*-Acetylglucosaminidase Reveals a Unique Asp-His Dyad Mechanism. *J. Biol. Chem.*, **2010**, *285*, 35675–35684. (b) Vocadlo, D. J.; Mayer, C.; He S.; Withers, S. G. Mechanism of Action and Identification of Asp242 as the Catalytic Nucleophile of *Vibrio furnisii N*-Acetyl-*β*-d-glucosaminidase Using 2-Acetamido-2-deoxy-5-fluoro-*α*-l-idopyranosyl Fluoride. *Biochemistry*, **2000**, *39*, 117–126. (c) Vocadlo D. J. ; Withers, S. G. Detailed Comparative Analysis of the Catalytic Mechanisms of β-*N*-Acetylglucosaminidases from Families 3 and 20 of Glycoside Hydrolases**.** *Biochemistry*, **2005**, *44*, 12809–12818.
12. Vocadlo D. J.; Davies, G. J. Mechanistic insights into glycosidase chemistry. *Curr. Opin. Chem. Biol.*, **2008**, *12*, 539–555.
13. (a) He, Y.; Macauley, M. S.; Stubbs, K. A.; Vocadlo D. J.; Davies, G. J. Visualizing the Reaction Coordinate of an O-GlcNAc Hydrolase. *J. Am. Chem. Soc.,* **2010**, *132*, 1807–1809. (b) Macauley, M. S.; Whitworth, G. E.; Debowski, A. W.; Chin D.; Vocadlo, D. J. *O*-GlcNAcase Uses Substrate-assisted Catalysis. *J. Biol. Chem.,* **2005**, *280*, 25313–25322.
14. Mark, B. L.; Vocadlo, D. J.; Knapp, S.; Triggs-Raine, B. L.; Withers S. G.; James, M. N. Crystallographic Evidence for Substrate-assisted Catalysis in a Bacterial β-Hexosaminidase. *J. Biol. Chem.,* **2001**, *276*, 10330–10337.
15. Elbatrawy, A. A.; Kim E. J.; Nam, G. *O*-GlcNAcase: Emerging Mechanism, Substrate Recognition and Small-Molecule Inhibitors, *ChemMedChem*, **2020**, *15*, 1244-1257.
16. Knapp, S.; Vocadlo, D.; Gao, Z.; Kirk, B.; Lou, J.; Withers, S. G. NAG-thiazoline, An *N*-Acetyl-β-hexosaminidase Inhibitor That Implicates Acetamido Participation. *J. Am. Chem. Soc*. **1996**, *118*, 6804–6805.
17. Macauley, M. S.; Whitworth, G. E.; Debowski, A. W.; Chin, D.; Vocadlo, D. J. O-GlcNAcase uses substrate-assisted catalysis: kinetic analysis and development of highly selective mechanism-inspired inhibitors. *J. Biol. Chem.* **2005**, *280*, 25313–25322.

18. Yuzwa, S. A.; Macauley, M. S.; Heinonen, J. E.; Shan, X.; Dennis, R. J.; He, Y.; Whitworth, G. E.; Stubbs, K. A.; McEachern, E. J.; Davies G. J.; Vocadlo, D. J. A potent mechanism-inspired O-GlcNAcase inhibitor that blocks phosphorylation of tau *in vivo*. *Nat. Chem. Biol.*, **2008**, *4*, 483–490.
19. Selnick, H. G.; Hess, J. F.; Tang, C.; Liu, K.; Schachter, J. B.; Ballard, J. E.; Marcus, J.; Klein, D. J.; Wang, X.; Pearson, M.; Savage, M. J.; Kaul, R.; Li, T.-S.; Vocadlo, D. J.; Zhou, Y.; Zhu, Y.; Mu, C.; Wang, Y.; Wei, Z.; Bai, C.; Duffy J. L.; McEachern, E. J. Discovery of MK-8719, a Potent O-GlcNAcase Inhibitor as a Potential Treatment for Tauopathies. *Journal of Medicinal Chemistry*, **2019**, *62*, 10062–10097.
20. Maaliki, C.; Gauthier, C.; Massinon, O.; Sagar, R. ; Vincent, S. P. Blériot Conformationally restricted glycoside derivatives as mechanistic probes and/or inhibitors of sugar processing enzymes and receptors *Carbohydr. Chem*., 2014, 40, 418–444
21. Hohenschutz, L. D.; Bell, E. A.; Jewess, P. J.; Ieworthy, D. P.; Price, R. J.; Arnold, E.; Clardy. J. Castanospermine, a 1,6,7,8- tetrahydroxyoctahydroindolizidine alkaloid, from seeds of Castanospermum australe. *Phytochemistry*, **1981**, *20*, 811-814.
22. García-Moreno, M. I.; Ortiz Mellet, C.; García Fernández, J. M. Polyhydroxylated *N*-(thio)carbamoylpiperidines: Nojirimycin-type glycomimetics with controlled anomeric configuration. *Tetrahedron: Asymmetry* **1999**, *10*, 4271–4275.
23. (a) Aydillo, C.; Navo, C. D.; Busto, J. H.; Corzana, F.; Zurbano, M. M.; Avenoza A.; Peregrina, J. M. A Double Diastereoselective Michael-Type Addition as an Entry to Conformationally Restricted Tn Antigen Mimics. *J. Org. Chem.,* **2013**, *78*, 10968–10977. (b) Venturi, F.; Venturi, C.; Liguori, F.; Cacciarini, M.; Montalbano M.; Nativi, C. A New Scaffold for the Stereoselective Synthesis of α-*O*-Linked Glycopeptide Mimetics. *J. Org. Chem.,* **2004**, *69*, 6153–6155. (c) Owens, N. W.; Braun, C.; Schweizer, F. Tuning of the Prolyl *trans*/*cis*-Amide Rotamer Population by Use of *C*-Glucosylproline Hybrids. *J. Org. Chem.,* **2007**, *72*, 4635–4643. (d) Mari, S.; Canada, F. J.; Jimenez-Barbero, J.; Bernardi, A.; Marcou, G.; Motto, I.; Velter, I.; Nicotra, F.; La Ferla, B. Synthesis and Conformational Analysis of Galactose-Derived Bicyclic Scaffolds. *Eur. J. Org. Chem.*, **2006**, 2925–2933.
24. a) Wang, H.; Luo, H, Ma, X.; Zou,W.; Shao, H. Stereoselective Synthesis of a Series of New *N*-Alkyl-3-hydroxypiperidine Derivatives Containing a Hemiketal, *Eur. J. Org. Chem.* **2011**, 4834–4840. b) La Ferla, B.; Bugada, P.; Cipolla, L.; Peri F.; Nicotra, F. Synthesis of Imino Sugar Scaffolds for the Generation of Glycosidase Inhibitor Libraries. *Eur. J. Org. Chem.*, **2004**, 2451–2470. c) Domingues, M.; Jaszczyk, J., Ismael, M.I., Figueiredo, J.A., Daniellou, R., Lafite, P., Schuler, M. and Tatibouët, A. (2020), Conformationally Restricted Oxazolidin-2-one Fused Bicyclic Iminosugars as Potential Glycosidase Inhibitors. *Eur. J. Org. Chem*., **2020**, 6109-6126.
25. Tikad, A.; Delbrouck J. A.; Vincent, S. P. Debenzylative Cycloetherification: An Overlooked Key Strategy for Complex Tetrahydrofuran Synthesis. *Chemistry - A European Journal*, **2016**, *22*, 9456–9476.
26. Cipolla, L.; Lay L.; Nicotra, F. New and Easy Access to C-Glycosides of Glucosamine and Mannosamine**.** *The Journal of Organic Chemistry*, **1997**, *62*, 6678–6681.
27. Hager, D.; Mayer, P. ; Paulitz, C. ; Tiebes J. ; Trauner, D. Stereoselective Total Syntheses of Herbicidin C and Aureonuclemycin through Late-Stage Glycosylation**.** *Angewandte Chemie International Edition*, **2012**, *51*, 6525–6528.
28. Peri, F.; Bassetti, R.; Caneva, E.; de Gioia, L.; La Ferla, B.; Presta, M.; Tanghetti E.; Nicotra, F. Arabinose-derived bicyclic amino acids: synthesis, conformational analysis and construction of an $\alpha_v\beta_3$-selective RGD peptide**.** *Journal of the Chemical Society, Perkin Transactions 1*, **2002**, 638–644.
29. Cipolla, L.; Forni, E.; Jiménez-Barbero J.; Nicotra, F. Synthesis and Conformational Analysis of Fructose- Derived Scaffolds: Molecular Diversity from a Single Molecule**.** *Chemistry - A European Journal*, **2002**, *8*, 3976–3983.
30. Cipolla, L.; La Ferla, B.; Peri F.; Nicotra, F. A new procedure for the synthesis of *C*-glycosides of nojirimycin. *Chemical Communications*, **2000**, 1289–1290.
31. Cipolla, L.; Palma, A.; La Ferla B.; Nicotra, F. Synthesis of nojirimycin *C*-glycosides. *Journal of the Chemical Society, Perkin Transactions 1*, **2002**, 2161–2165.
32. (a) Foucart, Q.; Marrot, J.; Désiré J.; Blériot, Y. Site-Selective Debenzylation of *C*-Allyl Iminosugars Enables Their Stereocontroled Structure Diversification at the C-2 Position**.** *Organic Letters*, **2019**, *21*, 4821–4825. (b) Foucart, Q.; Shimadate, Y.; Marrot, J.; Kato, A.; Désiré, J.; Blériot, Y. Synthesis and glycosidase inhibition of conformationally locked DNJ and DMJ derivatives exploiting a 2-oxo-C-allyl iminosugar. *Org. Biomol. Chem.* **2019**, *17,* 7204-7214.

33. Cekic, N.; Heinonen, J. E.; Stubbs, K. A.; Roth, C.; He, Y.; Bennet, A. J.; McEachern, E. J.; Davies G. J.; Vocadlo, D. J. Analysis of transition state mimicry by tight binding aminothiazoline inhibitors provides insight into catalysis by human O-GlcNAcase. *Chemical Science*, **2016**, *7*, 3742–3750.
34. Stubbs, K. A. ; Bacik, J.-P. ; Perley-Robertson, G. E. ; Gloster, T. M. ; Vocadlo D. J. ; Mark, B. L. The development of selective inhibitors of NagZ: increased susceptibility of Gram-negative bacteria to β-lactams. *ChemBioChem*, **2013**, *14*, 1973-1981.
35. Kong, H.; Chen, W.; Liu, T.; Lu, H.; Yang, Q.; Dong, Y.; Liang, X.; Jin S.; Zhang, J. Synthesis of NAM-thiazoline derivatives as novel O-GlcNAcase inhibitors. *Carbohydrate Research*, **2016**, *429*, 54–61.
36. Mondon, M.; Hur, S.; Vadlamani, G.; Rodrigues, P.; Tsybina, P.; Oliver, A.; Mark, B. L.; Vocadlo D. J.; Blériot, Y. Selective trihydroxyazepane NagZ inhibitors increase sensitivity of *Pseudomonas aeruginosa* to β-lactams. *Chemical Communications*, **2013**, *49*, 10983-10985.
37. Bergeron-Brlek, M.; Goodwin-Tindall, J.; Cekic, N.; Roth, C.; Zandberg, W. F.; Shan, X.; Varghese, V.; Chan, S.; Davies, G. J.; Vocadlo D. J.; Britton, R. A Convenient Approach to Stereoisomeric Iminocyclitols: Generation of Potent Brain-Permeable OGA Inhibitors**.** *Angewandte Chemie International Edition*, **2015**, *54*, 15429–15433.
38. Gloster, T. M.; Vocadlo, D. J. Mechanism, Structure, and Inhibition of *O*-GlcNAc Processing Enzymes. *Curr. Signal Transduct. Ther.* **2010**, *5*, 74–91.
39. Dvir, H.; Harel, M.; McCarthy, A. A.; Toker, L.; Silman, I.; Futerman, A. H.; Sussman, J. L. X-ray structure of human acid-beta-glucosidase, the defective enzyme in Gaucher disease. *EMBO reports*, **2003**, *4*, 704–709.
40. Vocadlo DJ, Mayer C, He S, Withers SG. Mechanism of action and identification of Asp242 as the catalytic nucleophile of Vibrio furnisii N-acetyl-beta-D-glucosaminidase using 2-acetamido-2-deoxy-5-fluoro-alpha-L-idopyranosyl fluoride. *Biochemistry*. **2000**, *39*, 117-126.
41. Balcewich MD, Stubbs KA, He Y, James TW, Davies GJ, Vocadlo DJ, Mark BL. Insight into a strategy for attenuating AmpC-mediated beta-lactam resistance: structural basis for selective inhibition of the glycoside hydrolase NagZ. *Protein Sci.* **2009**, *18*, 1541-1551.
42. Pickens, J. B. ; Wang, F. ; Striegler, S. Picomolar inhibition of β-galactosidase (bovine liver) attributed to loop closure. *Bioorganic & Medicinal Chemistry*, **2017**, *25*, 5194–5202.
43. Alvarez-Dorta, D.; King, D. T.; Legigan, T.; Ide, D. ; Idachi, I.; Deniaud, D.; Désiré, J.; Kato, A.; Vocadlo, D. J.; Gouin, S.; Blériot, Y. Multivalency to inhibit and discriminate hexosaminidases. *Chem. Eur. J.* **2017**, *23*, 9022-9025.
44. Howe JD, Smith N, Lee MJ, Ardes-Guisot N, Vauzeilles B, Désiré J, Baron A, Blériot Y, Sollogoub M, Alonzi DS, Butters TD. Novel imino sugar α-glucosidase inhibitors as antiviral compounds. *Bioorg Med Chem.* **2013**, *21*, 4831-4838.